2022-01-24

Macromolecular composition and substrate range of three marine fungi across major cell types

Thomas, S

10.1093/femsmc/xtab019
FEMS Microbes
Oxford University Press (OUP)

FEMS Microbes, 3, 2022, xtab019

https://doi.org/10.1093/femsmc/xtab019
Advance Access Publication Date: 24 January 2022
Research Article

RESEARCH ARTICLE – Microbes & Environment

Macromolecular composition and substrate range of three marine fungi across major cell types

Seth Thomas[1], Sabine K. Lengger[2], Kimberley E. Bird[1,†], Ro Allen[1] and Michael Cunliffe[1,3,*]

[1]Marine Biological Association, The Laboratory, Citadel Hill, Plymouth, PL1 2PB, UK, [2]School of Geography, Earth and Environmental Sciences, University of Plymouth, Plymouth, PL4 8AA, UK and [3]School of Biological and Marine Sciences, University of Plymouth, Plymouth, PL4 8AA, UK

*Corresponding author: Marine Biological Association, The Laboratory, Citadel Hill, Plymouth, PL1 2PB, UK. Tel: +44 (0)1752 426328; E-mail: micnli@mba.ac.uk
†Seth Thomas, https://orcid.org/0000-0001-7966-7526
‡Kimberley E. Bird, https://orcid.org/0000-0002-7244-5960
#Michael Cunliffe, https://orcid.org/0000-0002-6716-3555

ABSTRACT

Marine fungi exist as three major cell types: unicellular yeasts, filamentous hyphae and zoosporic early-diverging forms, such as the Chytridiomycota (chytrids). To begin to understand the ecological and biogeochemical influence of these cell types within the wider context of other plankton groups, cell size and macromolecular composition must be assessed across all three cell types. Using a mass–balance approach to culture, we describe quantitative differences in substrate uptake and subsequent macromolecular distribution in three model marine fungi: the yeast *Metschnikowia zobellii*, the filamentous *Epicoccum nigrum* and chytrid *Rhizophydium littoreum*. We compared these model cell types with select oleaginous phytoplankton of specific biotechnological interest through metanalysis. We hypothesise that fungal cell types will maintain a significantly different macromolecular composition to one another and further represent an alternative grazing material to bacterioplankton and phytoplankton for higher trophic levels. Assessment of carbon substrate range and utilisation using phenotype arrays suggests that marine fungi have a wide substrate range. Fungi also process organic matter to an elevated-lipid macromolecular composition with reduced-protein content. Because of their size and increased lipid composition compared to other plankton groups, we propose that fungi represent a compositionally distinct, energy-rich grazing resource in marine ecosystems. We propose that marine fungi could act as vectors of organic matter transfer across trophic boundaries, and supplement our existing understanding of the microbial loop and carbon transfer in marine ecosystems.

Keywords: marine fungi; lipid; protein; carbohydrate; allometry

INTRODUCTION

DNA-based surveys have revealed the diversity of the marine fungi (Amend *et al.* 2019; Gladfelter, James and Amend 2019), with Ascomycota and Basidiomycota, along with Chytridiomycota being the dominant phyla (Comeau *et al.* 2016; Hassett and Gradinger 2016; Taylor and Cunliffe 2016; Hassett *et al.* 2019). However, despite emerging evidence of their ecological importance (Gutiérrez *et al.* 2011; Gutiérrez, Jara and Pantoja

Received: 15 March 2021; **Accepted:** 25 November 2021

2016; Bochdansky, Clouse and Herndl 2017; Cunliffe *et al*. 2017; Grossart *et al*. 2019; Chrismas and Cunliffe 2020; Priest *et al*. 2021) our understanding of the functional roles of fungi in marine ecosystems remains limited (Amend *et al*. 2019).

Diversity studies indicate that marine fungi exist as three major cell types; unicellular yeasts, multicellular filamentous hyphae and as zoosporic early-diverging forms, mainly as Chytridiomycota (chytrids). Within these cell types are a range of distinct ecological and biogeochemical functions. Marine yeasts have similar morphology to bacteria but are an order of magnitude larger and encompass important functional groups, including invertebrate parasites (van Uden and Castelo-Branco 1961; Codreanu and Codreanu-Balcescu 1981). Filamentous fungi distributed throughout the water column may stabilise particles and as such could influence particulate organic carbon (POC) dynamics (Bochdansky, Clouse and Herndl 2017). Chytrids include phytoplankton parasites and potentially determine host community development and composition (Gutiérrez *et al*. 2011).

For well-studied plankton groups (e.g. phytoplankton), cell size or allometric differences account for a range of ecological processes, including nutrient uptake variability, ingestion and respiration (Moloney and Field 1989), cellular-scale and ecosystem wide metabolism (Sommer *et al*. 2017; Nidzieko 2018) and overall cellular carbon quota (Casey *et al*. 2019). Allometry can dictate the macromolecular composition of eukaryotic microorganisms through cell physiology, growth rate and investment in energy stores (Chan 1978; Hitchcock 1982; Moal *et al*. 1987). Fungal morphological diversity may similarly facilitate differentiation of their ecological niche and biochemical composition from other marine microbes, whilst simultaneously impacting organic matter transfer across trophic levels.

The biological carbon pump (BCP) removes more than 10 billion tonnes of carbon from the epipelagic zone each year (Buesseler and Boyd 2009), of which autochthonous particulate organic matter (POM) constitutes a significant proportion (Jiao *et al*. 2010). Bacteria are currently considered to dominate heterotrophic carbon cycling and uptake of autochthonous organic matter (Mühlenbruch *et al*. 2018). Heterotrophic microbial eukaryotes, though much less studied, can influence the composition and residence time of POM and therefore the efficacy of the BCP (Worden *et al*. 2015; Duret, Lampitt and Lam 2020). Sinking particles in the oceans are possible hotspots for fungi (Bochdansky, Clouse and Herndl 2017), and POC processing by fungi may reduce carbon sequestration to the deep ocean (Grossart *et al*. 2019), with the subsequent incorporation of POC-carbon into cellular macromolecules facilitating transfer through pelagic food webs.

At present, there is a limited understanding of the biochemical composition of marine fungi, particularly across the three major cell types. Distinctive amino acid, fatty acid and sterol compositions relative to other plankton, and which may be of specific benefit to fungi-consuming grazers, have recently been shown (Gutiérrez *et al*. 2020). Quantification of other major macromolecular groups and comparisons with other marine microbes, are still lacking. Differences in carbon resource allocation to specific macromolecules can determine the chemical energy potential of a cell, with lipid energy storage representing a significantly greater resource (9.50 kcal/g) than proteins (4.19 kcal/g) or carbohydrates (4.20 kcal/g; Prosser and Brown 1961; Hitchcock 1982). With phytoplankton, larger cells typically invest a greater proportion of carbon into lipid energy reserves (Finkel, Follows and Irwin 2016). However, large phytoplankton species often exhibit morphological or biochemical traits that convey a resistance to grazing (Wilson, Sarnelle and Tillmanns 2006). In the case of fungal cells, inherently larger allometries could increase their 'palatability' to grazers and the subsequent transfer of carbon and potential chemical energy to higher trophic levels.

If we are to fully understand the ecological and biogeochemical influence of marine fungal cell types, including within the wider context of other plankton groups, cell allometry and macromolecular composition must be comparatively assessed. We focused on three marine fungi that represent the major cell types and are prevalent at the Western Channel Observatory (WCO): the marine yeast *Metschnikowia zobellii*, the filamentous hyphal form *Epicoccum nigrum* and the chytrid *Rhizophydium littoreum,* in a mass-balance approach to trace incorporation of macronutrients into proteins, carbohydrates, lipids and nucleic acids. We further assessed the carbon substrate range of each taxa across 192 carbon sources of varying molecular weights.

MATERIALS AND METHODS

Metschnikowia zobellii and *E. nigrum* have a historical grounding in the field of marine mycology (van Uden and Castelo-Blanco 1961; Ahumada-Rudolph, Novoa and Becerra 2019). *Metschnikowia zobellii* MBA_F0073 and *E. nigrum* MBA_F0019 from the MBA Marine Fungi Culture Collection (MFCC) were maintained on marine Wickerham's yeast malt medium and potato dextrose medium respectively. DNA of the candidate strains was extracted using the DNEasy plant tissue kit (Qiagen, Germany) as per manufacturer instructions. The ITS region was amplified via PCR using ITSF1 and ITS4 primers (Eurofins, Luxembourg). Sanger sequencing (Source BioScience, Nottingham, UK) of PCR products was performed using forward and reverse primers. Forward and reverse reads were aligned using Geneious Prime (2021.0.3, Biomatters, Auckland, NZ) and a consensus sequence was extracted. Sequences were BLASTed against the NCBI-nr database with uncultured and environmental samples excluded, to confirm taxonomy as *M. zobellii* and *E. nigrum*.

As far as we are aware, *R. littoreum* is the only marine chytrid available in culture. *Rhizophidiales* have a wide spread distribution and are present across the Arctic Ocean, Baltic Sea, Bering Sea, Ligurian Sea and South Indian Ocean (Hasset *et al*. 2020). *Rhizophydium littoreum* was obtained from the American Type Culture Collection (ATCC 36100) and maintained on marine peptonised-milk, tryptone and glucose (PmTG) agar plates.

Triplicate cultures were grown in liquid media in 75 cm^3 tissue culture flasks (Sarstedt, Germany) at 15°C (aligning with the modal temperature at L4 Station over an 11-year period; Figure S1, Supporting Information), under a 14:10 light–dark cycle with continual mixing at 60 rpm. All strains, with the exception of *R. littoreum* zoospores, were grown in modified MAMS media supplemented with 20 mM glucose or N-acetyl-glucosamine (NAG). Prior to experimentation, cultures were washed twice by centrifugation at 4000 rpm (Megafuge 40R, Thermo Scientific, UK) for 10 min, the supernatant/media removed and the pellet resuspended in the same volume of carbon-free MAMS. To obtain zoospore samples, mature *R. littoreum* PmTG agar plates were flooded with 4 mL artificial seawater (3.5%; Sigma, UK) for 30 min. The released zoospores were passed through a 10 μm cell sieve to remove unwanted cellular detritus.

A timeline of culture growth and sample extraction is presented in Figure S2 (Supporting Information). Supernatants for substrate utilisation assays were harvested by centrifugation of 2 mL culture aliquots at 13 000 rpm for 5 min. Glucose depletion was quantified using a total reducing sugar assay (Dubois

et al. 1956). Triplicate samples of 0.5 mL of the culture supernatant were suspended in 2.5 mL of 1M H_2SO_4 and incubated at 121°C in an autoclave (Vario19, Dixons, UK) for 15 min. Samples were allowed to cool to room temperature before centrifugation at 4000 rpm for 10 min and 30 μL was gently mixed with 0.5 mL 4.0% phenol (v/v), further mixed with 2.5 mL of concentrated H_2SO_4 and again cooled to room temperature. A total of 200 μL of each sample were pipetted into a 96-well plate and absorbance measured (485 nm) using a CLARIOstar micro-plate reader (BMG Labtech, UK). NAG concentration was quantified using a commercial enzymatic D-glucosamine assay (K-GAMINE 04/18, Megazyme, Ireland) and ammonia was quantified using a commercial fluorescence assay (MAK310, Merck, UK), using harvested supernatants and following the manufacturer's instructions.

Carbon substrate range

Carbon substrate range was assessed in triplicate using Biolog PM1 and PM2A microarrays (Biolog, Hayward, CA), combining 192 substrates (Table S1, Supporting Information). Washed cells were resuspended in carbon-free MAMS media to a density of 10^3 cells/mL and 100 μL were added to each well plate. Plates were maintained under a 14:10 light–dark cycle at 15°C on an orbital shaker rotating at 60 rpm. Optical density was used as a proxy for growth over 72 h and measured (*R. littoreum* 495 nm; all others 600 nm) using a CLARIOstar micro-plate reader. The Shannon Diversity Index (henceforth, referred to as substrate diversity index) was calculated using the formula:

$$H = -N_{i=1}\, pi(lnpi),$$

where *pi* is the proportion of microbial activity on a substrate *I*, in this case growth rate/day and *N* is the number of substrates available (Fuentes and Quiñones 2016).

Biomass quantification

For growth experiments, biomass was estimated via optical density (*R. littoreum* 495 nm; Stevenson *et al.* 2013; all others 600 nm). Triplicate absolute biomass samples were also taken at mid-exponential (day 4) and stationary phase (day 6) for macromolecular analyses. A total of 50 mL of culture per time point were centrifuged at 4000 rpm for 10 min and the supernatant removed. The pellets were washed twice in 25 mL MilliQ water to remove media salts before storage at −80°C. After freeze-drying (Scan-Vac CoolSafe, LaboGene, Denmark) for 72 h at −50°C, dry-weight biomass was quantified.

Allometry

The allometry of fungal cell types was compared with the marine bacterium *Joostella* sp. for reference. Fungal cultures were stained with Calcofluor White (Sigma, UK; $\lambda = 360$ nm EX/460 nm EM) for cell wall visualisation. *Joostella* sp. cells were stained with MitoTracker Red (Thermo Fisher, Waltham, MA, USA; $\lambda =$ 579 nm EX/599 nm EM) for cell membrane visualisation. Both were also stained with Nile Red (Sigma; $\lambda = 552$ nm EX/636 nm EM) for qualitative lipid analysis. Images were captured using a Leica TCS SP8 DLS confocal microscope (Leica Microsystems, Germany). For estimations of cell volume, yeast and bacteria cells were treated as a capsule. For filamentous cells, a cylinder was used to calculate volume. In the case of chytrids, rhizoids were discounted from cellular volume calculations and a sphere was used for estimations.

Macromolecule quantification

The protein extraction was based on (Slocombe *et al.* 2013), with minor modifications. 3–5 mg of lyophilised biomass was rehydrated with 200 μL 24% (w/v) trichloroacetic acid (TCA), incubated at 95°C in an Eppendorf ThermoMixer C (Eppendorf, Stevenage, UK) and allowed to cool to room temperature. A total of 600 μL MilliQ water was added and samples centrifuged at 13 000 RPM for 5 min. Supernatants were discarded and the pellets were resuspended in 500 μL of 48:1:1 2% (w/v) Na_2CO_3 in 0.1N NaOH : 1% (w/v) $KNaC_4H_4O_6.4H_2O$: 0.5% (w/v) $CuSO_4.5H_2O$ in MilliQ water and incubated overnight at 55°C. Samples were then centrifuged at 13 000 rpm for 5 min, then 25 μL of the supernatant combined with 1 mL of the 48:1:1 reagent mix, homogenised *via* inversion and incubated at room temperature for 10 min. A total of 100 μL of a 1:1 mix of 2N Folin-Ciocalteu phenol reagent: MilliQ water was added to samples, immediately vortexed and then incubated for 30 min at room temperature. Protein content was measured *via* absorbance (600 nm) using a CLARIOstar micro-plate reader.

Lipid extraction and quantification were based on Bligh and Dyer (1959). Lyophilised samples were extracted in methanol (MeOH), dichloromethane (DCM) and phosphate-buffer (P) in a 2:1:0.8 (v/v/v) ratio, in an ultrasonic bath for 10 min. Extracted samples were centrifuged at 3000 rpm for 5 min. The supernatant was collected, and the remaining biomass was re-extracted twice. The combined supernatant was separated into two phases with the addition of DCM and P-buffer to achieve a new ratio of 1:1:0.9 (v/v/v). Phases were established by centrifuging samples at 3000 rpm for 2 min. The lower solvent phase was extracted, and the remaining upper phase was washed a further two times with DCM. All lower solvent phases were collected and evaporated under oxygen-free nitrogen (OFN) in a 25°C water bath (N-EVAP, Organomation, West Berlin, MA, USA). Dried extracts were weighed to quantify the total weight of lipids.

DNA and RNA concentrations were quantified fluorometrically using a Qubit 4 Fluorometer (Invitrogen, Thermo Fisher Scientific, UK). Culture aliquots of 1 mL were decanted in triplicate into 1.5 mL lysis tubes containing 5 mg of 212–300 nm diameter glass beads. Cells were lysed over 2 cycles at 6 m/s for 40 s using a FastPrep-24 5G homogeniser (MP Bioemedicals LLC, Germany). After centrifugation at 13 000 rpm for 2 min, nucleic acids were quantified using dsDNA HS Assay and RNA HS Assay Kits (Thermo Fisher Scientific) following the manufacturer's instructions.

Carbohydrates were quantified using the reducing sugars assay described above (Dubois *et al.* 1956; Slocombe *et al.* 2015) with 3–5 mg of lyophilised biomass.

Fatty acid analysis

Bligh–Dyer extracts were dissolved in DCM and loaded onto a preactivated silica gel (4 h at 150°C) column for separation. Total lipid extracts were eluted into three fractions resulting from washing with one volume of DCM, one volume of acetone and two volumes of MeOH. Each fraction was evaporated to dryness under OFN. Acetone and MeOH fractions were rehydrated in 9:1 DCM: MeOH (v/v), combined and again evaporated to dryness. The resultant fatty acid extracts were transesterified in 0.561 g potassium hydroxide, 75 mL MeOH and 25 mL toluene at 37°C

for 1 h. 0.8 mL of MilliQ water were added to fatty acid methyl esters (FAMEs), which were subsequently separated using 75 mM acetic acid and DCM. FAME extracts were evaporated to dryness under OFN and suspended in 75 μL of hexane.

FAME samples were analysed by gas chromatography mass spectrometry (GCMS) using an Agilent 7890A GC coupled to an Agilent 5975C Inert XL MSD. A total of 1 μL of the samples dissolved in hexane were injected in splitless mode at 250°C onto an Agilent DB-5ms (30 m × 0.25 mm × 0.25 μm) column using helium as a carrier gas (1 mL/min; constant flow mode). The Agilent 7890A GC oven was programmed from 70 (1 min hold) to 130°C at 20°C/min, followed by a 5°C/min ramp to 300°C (15 min isothermal hold). The transfer line was held at 250°C, the source was kept at 230°C and the quadrupole at 150°C. Mass spectra were acquired at *m/z* 50–650. FAMEs were identified based on retention times and mass spectral comparisons with spectra from the methyl ester archive hosted at www.lipidhome.co.uk/ms/methesters/me-arch/index.htm.

Statistical analyses

Statistical analyses and data visualisations were conducted in RStudio ((R version 4.03) RStudio version 1.41.103, Boston, MA) with significance reported to $P < 0.05$ unless otherwise stated. Normal distributions were confirmed using Shapiro–Wilks tests. ANOVAs with TukeyHSD *post-hoc* tests were used to test for significant differences between treatments and species. Shannon Diversity indices were calculated in the package *vegan* (Oksanen *et al*. 2020). All data visualisations were crafted using *ggplot2* (Wickham 2016) and large panels were collated using the *patchwork* package.

RESULTS

Ecological prevalence of selected marine fungi

Metschnikowia zobellii and *E. nigrum* were prevalent throughout the 5-year time series that comprised the WCO DNA-based database (Taylor and Cunliffe 2016), each with instances of high relative abundance (Fig. 1). *Rhizophydium* sp. was less prevalent across the time-series, however, the ecology and physiology of this genus has been examined in other studies (Gleason *et al*. 2017; Raghukumar 2017; Scholz *et al*. 2017).

Allometry

Cell allometries were determined using fluorescence microscopy (Fig. 2), with cell volumes calculated depending on the specific cellular morphotype (Table 1). *Metschnikowia zobellii* showed an average diameter and volume of 7.9 ±0.7 μm and 28.1 ±1.0 μm^3, compared with *E. nigrum* 43.4 ±7.4 μm and 444.2 ±43.7 μm^3 and *R. littoreum* 14.5 ±3.3 μm and 1892.28 ± 519.9 μm^3, respectively (Fig. 2).

Nile red staining showed lipid compartments in the marine fungi (Fig. 2A–C). Lipid localisation in the mature *R. littoreum* zoosporangia indicate individual zoospores. Lipid localisation appears also in the *R. littoreum* rhizoid, which to our knowledge has not been reported previously. Lipid storage within the rhizoids may indicate utilisation as an endogenous energy source for rhizoid development.

Table 1. The macromolecular composition of marine fungi and bacteria, per gram of C and N assimilated, resultant potential chemical energy and cellular allometry. Error values represent ± 1 standard error from the mean (min. $n = 3$).

Species	C uptake rate (per day)	N uptake rate (per day)	Protein (g)	Carbohydrate (g)	Lipid (g)	DNA (mg)	RNA (mg)	Chemical energy (j/g)	Cell volume (μm^3)
Fungi									
M. zobellii	0.61 ± 0.01	0.19 ± 0.01	0.05 ± < 0.001	0.45 ± 0.03	0.46 ± 0.04	0.03 ± < 0.001	0.07 ± < 0.001	0.92 ± 0.05	28.1 ± 1.0
E. nigrum	0.10 ± 0.02	0.06 ± 0.02	0.01 ± < 0.001	0.22 ± 0.03	0.45 ± 0.02	0.001 ± < 0.001	0.39 ± 0.01	1.38 ± 0.08	444.2 ± 43.7
R. littoreum	0.16 ± 0.02	0.18 ± 0.09	0.02 ± < 0.001	0.01 ± < 0.01	0.71 ± 0.02	0.08 ± < 0.001	0.54 ± 0.01	1.29 ± 0.04	1892.3 ± 519.9

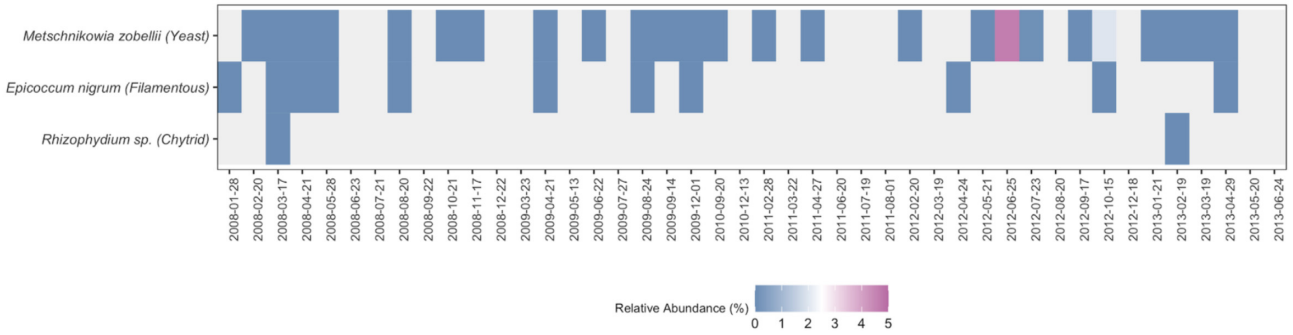

Figure 1. Relative abundance of *M. zobellii*, *E. nigrum* and *R. littoreum* at the WCO over a 5-year period. Data from Taylor and Cunliffe (2016).

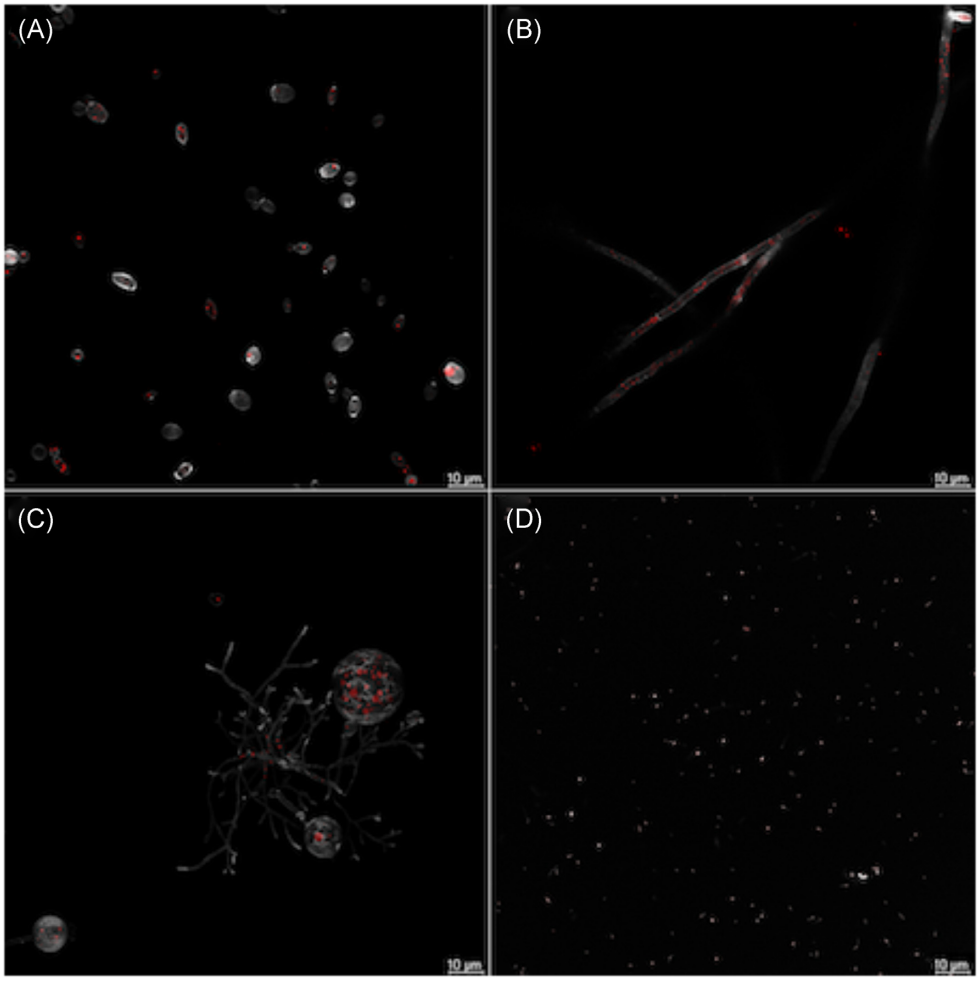

Figure 2. Marine fungi are orders of magnitude larger than bacteria and exhibit cellular compartmentalisation of lipids. Fluorescent labelling of cell wall structures (Calcofluor White) and cellular lipid content (Nile Red) for qualitative analysis of **(A)** *M. zobellii* **(B)** *E. nigrum*, **(C)** *R. littoreum* and **(D)** *Joostella sp.* (MitoTracker Red opposed to Calcofluor white). Scale bar = 10 μm.

Carbon substrate range

The fungi showed decoupling of growth rate and yields across the carbon substrates tested, with variable growth rates yet relatively constrained yields (Fig. 3). *Metschnikowia zobellii* exhibited the highest growth rate with fructose and growth yield with chondroitin sulfate C, compared with gluconic acid and amino valeric acid for *E. nigrum*, and glucose and acetoacetic acid for *R. littoreum*. No significant effect of carbon substrate type on growth rate or yield were found in either *M. zobellii* or *E. nigrum*. However, a significant effect of substrate type on both growth rate ($F = 2.09$, $P = 0.02$) and yield ($F = 2.76$, $P < 0.01$) with *R. littoreum* was observed and was attributed to the ester substrate group (Tukey HSD, $P < 0.01$). *Metschnikowia zobellii* and *E. nigrum* exhibited significantly enhanced growth rates on all carbon source types compared to *R. littoreum* (MANOVA, $F = 248.19$, $P < 0.01$; Fig. 4C).

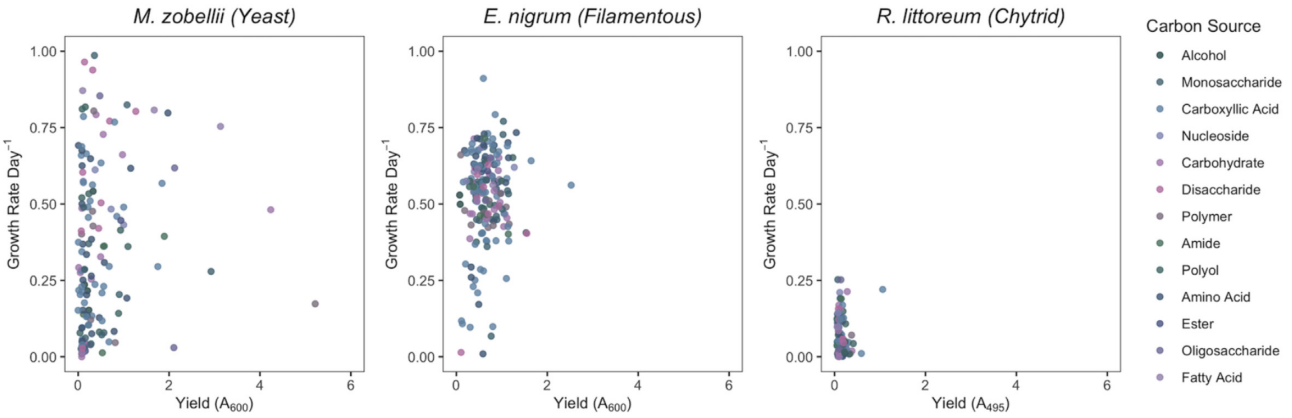

Figure 3. Marine fungi demonstrate growth-rate yield decoupling. Growth rate and yield for *M. zobellii*, *E. nigrum* and *R. littoreum*. Carbon sources are differentiated and coloured by molecule type. A_{600} refers to the wavelength used in optical density measurements.

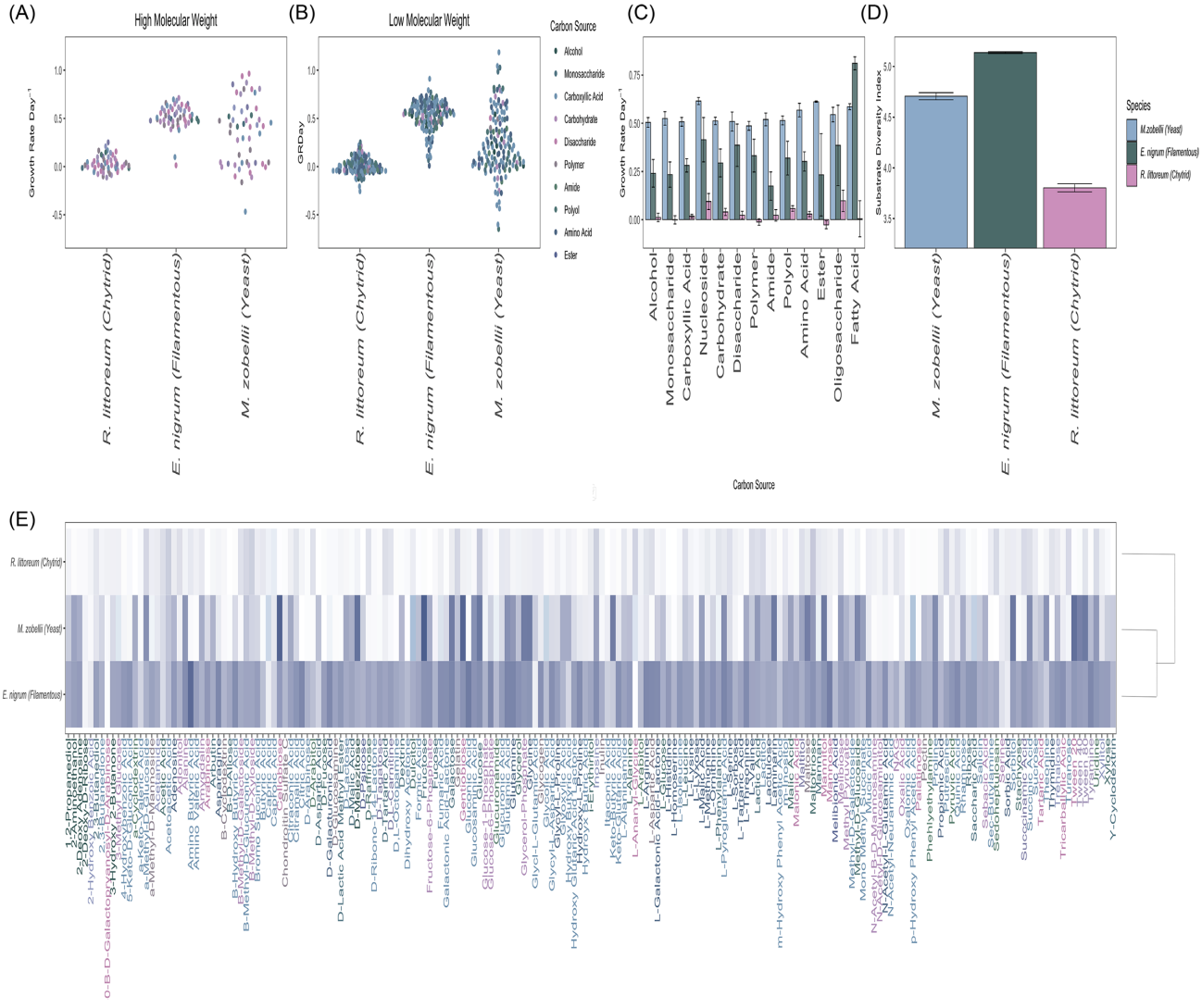

Figure 4. Ascomycota exhibit greater growth across a variety of carbon source types and molecular weights, and are differentiated from chytrids. Growth rate/day of considered taxa on HMW substrates (> 250 g/mol; $n = 3$). **(B)** Growth rate/day of considered taxa on LMW substrates (< 250 g/mol; $n = 3$). Each data point represents the mean of an individual carbon source, coloured by molecule type ($n = 3$). **(C)** Growth rate/day of model marine fungi across 13 carbon source types on phenotypic microarrays (mean ± 1 SE). **(D)** Substrate Diversity Index of considered species. Growth rate/day on individual substrates was used as a measure of activity and assesed across 192 substrates. ($n = 3$, mean ± 1 SE). **(E)** Euclidean distancing hierarchical clustering of growth rate/day of each taxa over 192 carbon sources ($n = 3$).

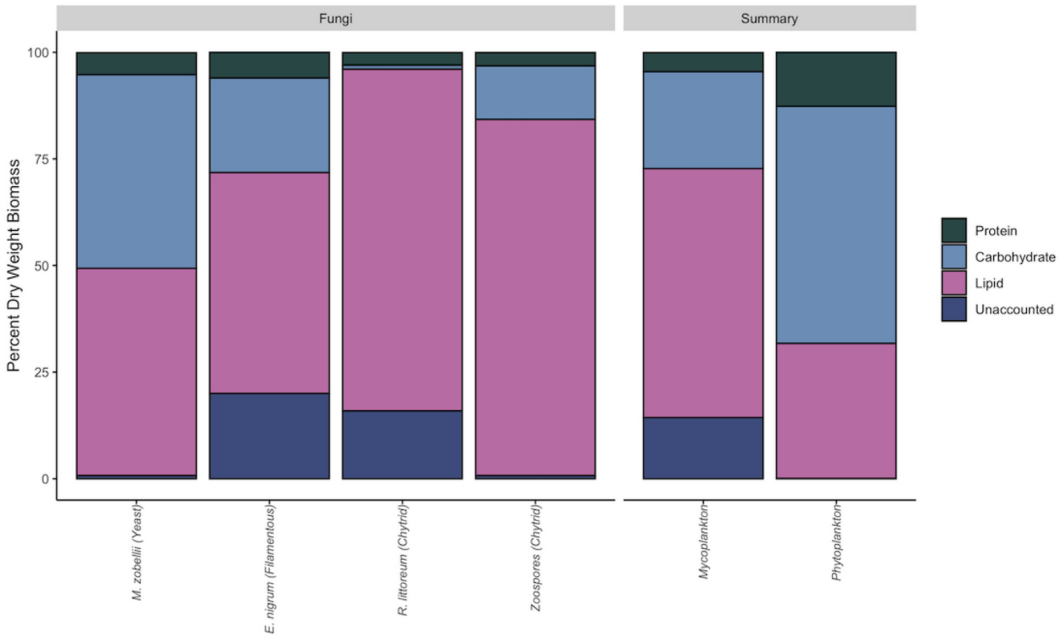

Figure 5. Marine fungi exhibit elevated lipid and reduced protein content compared to select phytoplankton. The macromolecular composition of marine fungal taxa as the percentage of dry weight biomass ($n = 9$). Summary panel reveals the average of taxa at the kingdom level. Phytoplankton data are consolidated from the literature (Supplementary Data 1, Slocombe *et al.* 2015; $n = 22$).

The Substrate Diversity Index was used to assess activity (growth rate/day) over all carbon substrates and revealed a wide substrate range of fungi in keeping with other fungal taxa (Zak *et al.* 1994; Tam *et al.* 2001; Muńiz *et al.* 2014). *Epicoccum nigrum* has the highest substrate diversity (H' 5.14 ± 0.01) followed by *M. zobellii* (H' 4.70 ± 0.03) and *R. littoreum* (H' 3.80 ± 0.04; Fig. 4D).

Carbon usage efficacy was also assessed with substrates separated as high molecular weight (HMW; > 250 g/mol) and low molecular weight (LMW; < 250 g/mol). *Metschnikowia zobellii* and *E. nigrum* exhibited the broadest range of growth rates across both HMW and LMW substrates (Fig. 4A and B), compared to *R. littoreum*.

Euclidean distance hierarchical clustering was used to examine the general relationship between the carbon substrate ranges of the different taxa (Fig. 4E) and showed that the substrate range of *M. zobellii* and *E. nigrum* clustered closely together and were differentiated from *R. littoreum*. Distinctive clustering of the two Ascomycota is indicative of similar capacities for degrading specific carbon substrates relative to other taxa and therefore indicates potential niche differentiation in natural ecosystems.

Substrate conversion to macromolecules

Metschnikowia zobellii grew more efficiently than *E. nigrum* and *R. littoreum* with glucose, completely depleting the substrate within 3 days (Figure S3, Supporting Information), demonstrating carbon limitation. Greater carbon uptake and concurrent reductions in uptake of ammonia in *E. nigrum* and *R. littoreum* during NAG incubations suggests that the fungi are capable of utilising NAG as a source of both carbon and nitrogen during heterotrophic growth. No significant effect of carbon substrate on final macromolecular composition of fungi was found.

Carbon substrate and ammonia uptake were converted from mM to grams to apply a mass balance approach to macromolecular composition (Table 1). As chytrid zoospores were cultivated on PmTG plates, directly measuring carbon and nitrogen uptake was not possible, so only percentage composition of macromolecules by dry weight biomass is reported. The macromolecular composition of phytoplankton by dry weight biomass was collated from other studies (Supplementary Data 1). The percentage dry weight composition of macromolecules in fungi was different from values reported for oleaginous phytoplankton in the literature (Fig. 5). Protein and carbohydrate composition were significantly lower in fungi compared to phytoplankton ($F = 34.9$, $P < 0.01$), however, lipid composition was significantly higher in fungi ($F = 27.7$, $P < 0.01$).

Rhizophydium littoreum exhibited the greatest proportion of lipids ($F = 4.95$, $P < 0.01$; Table 1) and the lowest proportion of carbohydrates. However, the zoospores of *R. littoreum* exhibit a significantly higher proportion of carbohydrates than mature zoosporangia ($F = 14.75$, $P < 0.01$). *Metschnikowia zobellii* showed the greatest carbon investment into carbohydrates, constituting a significantly greater carbohydrate allocation than all other fungal cell types. No significant differences were found in protein composition between any of the fungal species tested.

FAME composition

Ascomycota species were enriched with the canonical fungal fatty acid biomarkers C16:0, C16:1ω7, C18:1ω9, C18:2ω6 and C18:3ω6 (Fig. 6A and B). In addition to traditional fungal fatty acids, *R. littoreum* exhibited signatures from C14:0, C20:1, two species of C20:2 (one of those likely ω9), C20:3ω6, two species of C20:4, (one of those likely ω6) and C22:0 fatty acids (Fig. 6C). In addition, *M. zobellii* contained what is likely a diunsaturated cyclic C18 fatty acid (labelled as 'Unknown-A', retention time 19.8 min). Clustering of well-characterised polyunsaturated eicosanoate fatty acids exclusive to chytrids conveys their practicality as biomarkers for ecological studies in marine environments. Odd-chain polyenoic fatty acids noted in freshwater chytrid species (Akinwole, Lefevre and Powell 2014), but not

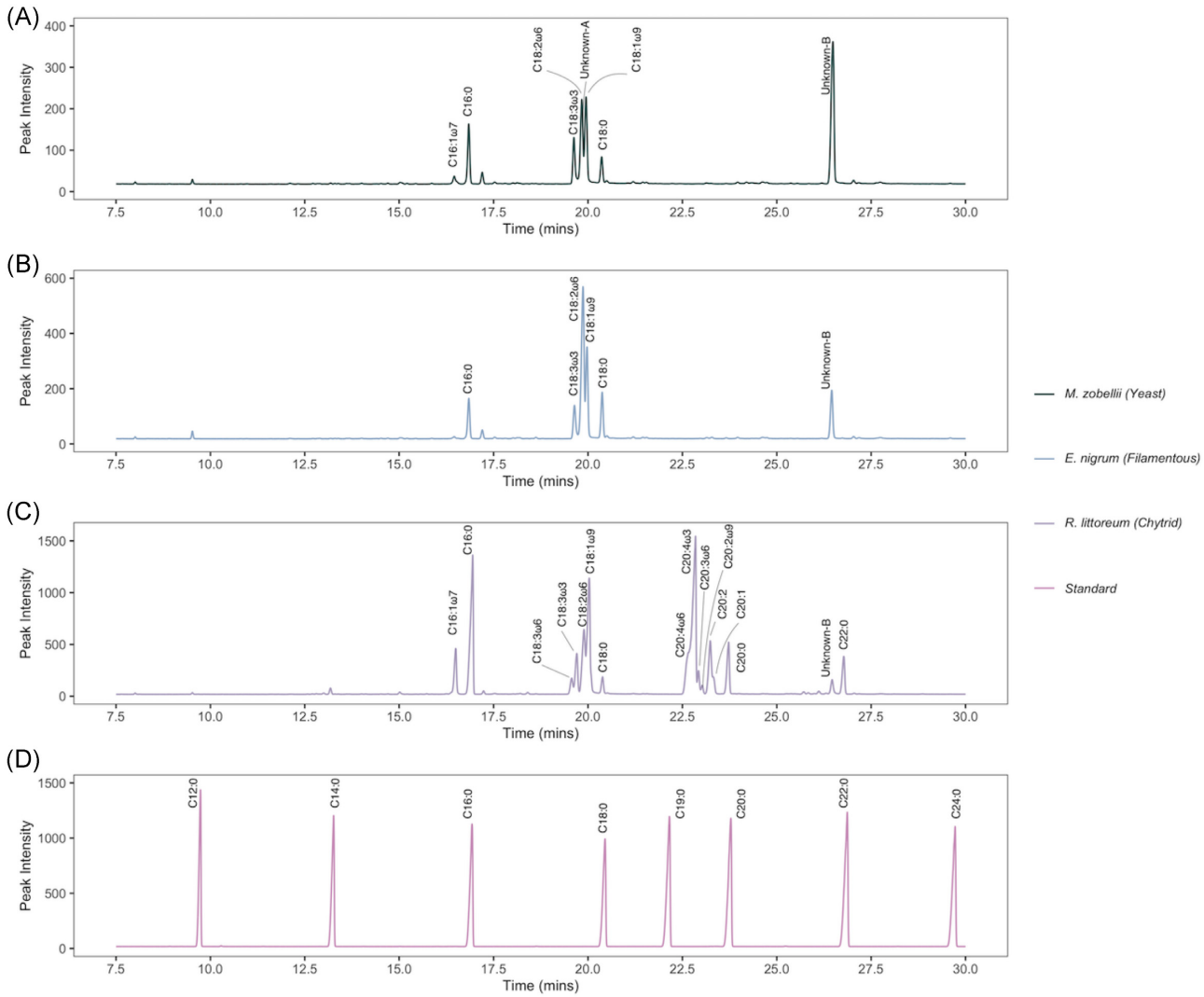

Figure 6. Mature zoosporangia of *R. littoreum* are enriched in C20 unsaturated fatty acids not present in Ascomycota species. Qualitative analyses of *M. zobellii* **(A)**, *E. nigrum* **(B)** and *R. littoreum* **(C)** FAME profiles. FAMEs were identified based on retention times and mass spectra relative to a standard mix **(D)**.

known to occur in higher fungi, were not observed in here. An unknown compound which may be a phenyl-functionalised fatty acid (labelled as 'Unknown-B') was found across all investigated taxa. However, ubiquity of this atypical fatty acid across taxa may indicate a low level contaminant and warrants further investigation.

DISCUSSION

Fungi exhibit an uncoupling of growth rate and final growth yield (Fig. 3) which could be explained by investment in cellular resources, such as storage lipids, as opposed to cellular division (Lipson 2015). Marine fungi may also divert cellular resources to salinity stress responses. In the marine fungus *Paradendryphiella salina,* growth under increased salinities results in the greater investment into production of compatible solutes (Paton and Jennings 1988) and increased cell wall thickness (Clipson, Jennings and Smith 1989) at the cost of cell division (Jennings and Burke 1990). Investment of carbon in this manner (i.e. cell sustainment as opposed to reproduction) would limit changes to optical density within the phenotypic microarrays and, thus offer a possible explanation for the observed uncoupling between growth rate and yield.

Yeast and filamentous cell types have a wider substrate range than chytrids (Fig. 4D), with hierarchical clustering showing significant differences between the carbon assimilation and corresponding growth rates of the marine Ascomycota (*M. zobelli* and *E. nigrum*) and *R. littoreum* (Fig. 4E). Differentiation in carbon substrate usage is further supported by greater success of *M. zobellii* and *E. nigrum* on HMW substrates in comparison to *R. littoreum*. Given the proclivity for HMW substrates demonstrated here by the Ascomycota, and the specialisation of these fungi to HMW plant-derived biopolymers observed in terrestrial systems (Algora Gallardo, Baldrian and López-Mondéjar 2021), the functional roles of fungal cell types may differ in the marine environment. Future studies will need to expand this approach to characterise substrate ranges of a broader diversity of marine fungi and comparisons to model phytoplankton and bacteria, both in terms of culture-based experiments as here and with culture-independent approaches.

Marine snow particles are hot spots for fungi (Bochdansky, Clouse and Herndl 2017). Particle-attached microbes mediate carbon cycling in the aquatic environment by degrading

insoluble HMW POM. Particle degradation dynamics follow a modular assembly of two subsequent functional groups; (i) narrowly specialised primary degraders, whose dynamics are controlled by POM composition; and (ii) substrate independent taxa, whose dynamics are controlled by interspecific interactions (Enke *et al.* 2019). The apparent specialisation in utilising HMW substrates tentatively suggests that marine fungi may be primary particle degraders. This functional role has been further substantiated by analysis of the Tara Ocean eukaryote metatranscriptome database, which showed a high prevalence of glycoside hydrolase genes transcribed attributed to Ascomycota, indicating widespread *in situ* degradation of HMW substrates typical of POM in the open ocean (Chrismas and Cunliffe 2020).

We quantitatively describe the macromolecular composition of marine fungi as significantly different to select oleaginous phytoplankton (Slocombe *et al.* 2015). In the marine fungi assessed here, carbohydrates are significantly lower and lipids significantly greater than in oleaginous phytoplankton, and together drive an elevated potential chemical energy content in fungi. Protein content is significantly reduced in fungi relative to oleaginous phytoplankton, however, may still represent a distinct resource to grazers due to an enrichment of specific amino acids histidine, threonine, valine, lysine and leucine (Gutiérrez *et al.* 2020). On average, fungi possess a lipid: carbohydrate: protein ratio of *c.* 13:5:1 (g/g/g). Importantly, these differences occur over orders of allometric magnitude, placing fungi in the varying preferential grazing size ranges from heterotrophic flagellates to zooplankton (Sommer *et al.* 2000). Therefore, with high lipid and high carbohydrate composition, fungi may constitute a valuable resource for grazers in marine ecosystems.

Macromolecular analysis revealed an exceptional lipid-majority in the zoosporangia and zoospores of the marine chytrid *R. littoreum*. In freshwater ecosystems, chytrids zoospores are at densities comparable to the carbon biomass of significantly larger filamentous fungi and bacterial communities (Kagami, Helmsing and van Donk 2011). When combined with parasitism-mediated release, chytrid-associated carbon can account for as much as 11% of dissolved organic carbon (DOC) and 69% of POC (Gutiérrez, Jara and Pantoja 2016). Chytrid parasitism of phytoplankton can enhance herbivory in pelagic food webs by fragmenting large cells, rendering phytoplankton more edible (Frenken *et al.* 2020) These interactions have made inaccessible carbon (e.g. large inedible diatoms) directly available to freshwater zooplankton grazers via the mycoloop (Kagami, Miki and Takimoto 2014).

Diversity and abundance of mycoplankton are correlated with that of phytoplankton (Taylor and Cunliffe 2016; Kilias *et al.* 2020; Priest *et al.* 2021). The apparent constitutive lipid contents of the fungi investigated here are significantly higher than in select oleaginous phytoplankton (Slocombe *et al.* 2015), and thus where available may represent a preferable feeding resource. Specific lipid composition may be a determinant in selective feeding by zooplankton and may effectively supplement a phytoplankton-based diet. All investigated fungi are rich in established saprotrophic fungal FAME biomarkers C16:0, C18:1ω9, C18:2ω6 and C18:3ω3, similar to fungi in non-marine aquatic ecosystems (Taube *et al.* 2019), and in agreement with the marine fungal isolates characterised by Gutierrez *et al.* (2020). However, *R. littoreum* is enriched with a cluster of longer C20 FAMEs absent in the Ascomycota and not previously identified in marine fungi. Chytrid specific FAMEs have been identified in aquatic ecosystems (Akinwole, Lefevre and Powell 2014), but are yet to be investigated in marine assemblages. These FAMEs, particularly C20:4ω3, are strong candidates for identification of active chytrids in marine systems. Several studies have described the fatty acid content of terrestrial (Gaspar, Pollero and Cabello 1994; Olsson 1999; Willers, van Rensburg and Claassens 2015) and more recently in freshwater and marine fungi (Gerphagnon *et al.* 2019; Taube *et al.* 2019; Gutiérrez *et al.* 2020). Reproductive success of the marine copepods *Acartia tonsa* and *Acartia hudsonica* were correlated with concentrations of C16:1ω7 (negative) and C18 fatty acids (Jønasdøttir 1994), of which marine fungi are a significant source (Taube *et al.* 2019; Gutiérrez *et al.* 2020). Further, these polyunsaturated fatty acids are widely considered as ecologically high-quality nutrients, and are specifically and preferentially maintained in *Calanus* copepods when available in grazing material (Parrish, French and Whiticar 2012).

The attained high growth rates and yields in optimal conditions, as well as the macronutrient uptake efficiencies of fungi shown here, raise questions about the constraints on fungal abundance in marine ecosystems. A high patchiness of resources within the marine environment (Grünbaum 2012), investment of carbon into cellular stress responses opposed to cell division (Clipson, Jennings and Smith 1989; Jennings and Burke 1990) and wide distribution of spores away from the immediate local environment may limit fungal abundance locally. However, abundance may also be constrained *via* selective feeding by grazers. Copepods represent a key linkage between marine microbes and higher trophic levels. The allometry of *M. zobellii* and *R. littoreum* are within the optimum particle size for grazing by copepods of 15 μm (Sommer *et al.* 2000) and molecular evidence of zooplankton grazing of mycoplankton is increasing. For example, metabarcoding analyses of *Calanus* copepod gut contents has revealed a high prevalence of Pezizomycotina (Ascomycota) and Agaricomycetes (Basidiomycota) (Ray *et al.* 2016; Yeh *et al.* 2020). Top-down grazer control would support the killing the winner hypothesis (Winter *et al.* 2010) by which the most effective or successful carbon assimilator is constrained by predation.

Here, we have demonstrated quantitatively the substrate range of prevalent marine fungi across the major cell types, and reveal comparable growth efficiency across LMW and HMW substrates. In addition, we have shown that incorporated substrates are processed to an energy-rich, lipid-majority macromolecular composition that supports a greater potential chemical energy content. Though the finite number of investigated taxa preclude wide-scale biogeochemical conclusions. Through their macromolecular composition, taken together with an accessible allometry and specific dietary benefits for zooplankton grazers, we suggest that marine fungi may have a functional role in processing recalcitrant HMW organic matter, such as that typical of marine POC, into more readily accessible carbon that may be disseminated up trophic boundaries. We add to the growing body of evidence that fungi perform unique and important functions that supplement our existing understanding of the microbial loop and carbon transfer in marine ecosystems.

FUNDING

All authors are supported by the European Research Council (ERC; MYCO-CARB project: grant number 772584).

SUPPLEMENTARY DATA

Supplementary data are available at *FEMSMC* online.

DATA AVAILABILITY

All data are available from the corresponding authors.

AUTHOR CONTRIBUTIONS

S.T. and M.C. conceived the study. S.T. conducted the laboratory work and data analysis. S.L. advised on lipid extraction procedures, carried out instrumental analysis and advised on lipid data analysis. K.B. and R.A. assisted with preliminary laboratory work and data analysis respectively. S.T. and M.C. interpreted and assessed the findings. S.T. and M.C. wrote the manuscript, with the help of S.L. K.B. and R.A.

ACKNOWLEDGEMENTS

The authors would like to thank Davis Laundon for his assistance with microscopy.

Conflicts of interest. None declared.

REFERENCES

Ahumada-Rudolph R, Novoa V, Becerra J. Morphological response to salinity, temperature, and pH changes by marine fungus *Epicoccum nigrum*. *Environ Monit Assess* 2019;**191**. https://link.springer.com/article/10.1007%2Fs10661-018-7166-5.

Akinwole PO, Lefevre E, Powell MJ *et al.* Unique odd-chain polyenoic phospholipid fatty acids present in chytrid fungi. *Lipids* 2014;**49**:933–42.

Algora Gallardo C, Baldrian P, López-Mondéjar R. Litter-inhabiting fungi show high level of specialization towards biopolymers composing plant and fungal biomass. *Biol Fertil Soils* 2021;**57**:77–88.

Amend A, Burgaud G, Cunliffe M *et al.* Fungi in the marine environment: open questions and unsolved problems. *MBio* 2019;**10**:e01189–18.

Bligh EG, Dyer WJ. A rapid method of total lipid extraction and purification. *Can J Biochem Physiol* 1959;**37**:911–7.

Bochdansky AB, Clouse MA, Herndl GJ. Eukaryotic microbes, principally fungi and labyrinthulomycetes, dominate biomass on bathypelagic marine snow. *ISME J* 2017;**11**:362–73.

Buesseler KO, Boyd PW. Shedding light on processes that control particle export and flux attenuation in the twilight zone of the open ocean. *Limnol Oceanogr* 2009;**54**:1210–32.

Casey JR, Björkman KM, Ferrón S *et al.* Size dependence of metabolism within marine picoplankton populations. *Limnol Oceanogr* 2019;**64**:1819–27.

Chan AT. Comparative physiological study of marine diatoms and dinoflagellates in relation to irradiance and cell size. I. Growth under continuous light. *J Phycol* 1978;**14**:396–402.

Chrismas N, Cunliffe M. Depth-dependent mycoplankton glycoside hydrolase gene activity in the open ocean: evidence from the Tara Oceans eukaryote metatranscriptomes. *ISME J* 2020:1–5. DOI: 10.1038/s41396-020-0687-2.

Clipson NJW, Jennings DH, Smith JL. The response to salinity at the microscopic level of the marine fungus *Dendryphiella salina* Nicot and Pugh as investigated stereologically. *New Phytol* 1989;**113**:21–7.

Codreanu R, Codreanu-Balcescu D. On two *Metschnikowia* yeast species producing hemocoelic infections in *Daphnia magna* and *Artemia salina* (Crustacea, Phyllopoda) from Romania. *J Invertebr Pathol* 1981;**37**:22–7.

Comeau AM, Vincent WF, Bernier L *et al.* Novel chytrid lineages dominate fungal sequences in diverse marine and freshwater habitats. *Sci Rep* 2016;**6**:1–6.

Cunliffe M, Hollingsworth A, Bain C *et al.* Algal polysaccharide utilisation by saprotrophic planktonic marine fungi. *Fung Ecol* 2017;**30**:135–8.

Dubois M, Gilles KA, Hamilton JK *et al.* Colorimetric method for determination of sugars and related substances. *Anal Chem* 1956;**28**:350–6.

Duret MT, Lampitt RS, Lam P. Eukaryotic influence on the oceanic biological carbon pump in the Scotia Sea as revealed by 18S rRNA gene sequencing of suspended and sinking particles. *Limnol Oceanogr* 2020;**65**:S49–70.

Enke TN, Datta MS, Schwartzman J *et al.* Modular assembly of polysaccharide-degrading marine microbial communities. *Curr Biol* 2019;**29**:1528–35.

Finkel Zv, Follows MJ, Irwin AJ. Size-scaling of macromolecules and chemical energy content in the eukaryotic microalgae. *J Plankton Res* 2016;**38**:1151–62.

Frenken T, Wolinska J, Tao Y *et al.* Infection of filamentous phytoplankton by fungal parasites enhances herbivory in pelagic food webs. *Limnol Oceanogr* 2020;**65**:2618–26.

Fuentes ME, Quiñones RA. Carbon utilization profile of the filamentous fungal species *Fusarium fujikuroi*, *Penicillium decumbens*, and *Sarocladium strictum* isolated from marine coastal environments. *Mycologia* 2016. DOI: 10.3852/15-338.

Gaspar ML, Pollero RJ, Cabello MN. Triacylglycerol consumption during spore germination of vesicular-arbuscular mycorrhizal fungi. *J Am Oil Chem Soc* 1994;**71**:449–52.

Gerphagnon M, Agha R, Martin-Creuzburg D *et al.* Comparison of sterol and fatty acid profiles of chytrids and their hosts reveals trophic upgrading of nutritionally inadequate phytoplankton by fungal parasites. *Environ Microbiol* 2019;**21**:949–58.

Gladfelter AS, James TY, Amend AS. Marine fungi. *Curr Biol* 2019;**29**:R191–5.

Gleason FH, Scholz B, Jephcott TG *et al.* Key ecological roles for zoosporic true fungi in aquatic habitats. *Microbiology Spectrum* 2017:399–416. DOI: 10.1128/microbiolspec.FUNK-0038-2016.

Grossart HP, van den Wyngaert S, Kagami M *et al.* Fungi in aquatic ecosystems. *Nat Rev Microbiol* 2019;**17**:339–54.

Grünbaum D. The logic of ecological patchiness. *Interface Focus* 2012;**2**:150–5.

Gutiérrez MH, Jara AM, Pantoja S. Fungal parasites infect marine diatoms in the upwelling ecosystem of the Humboldt current system off central Chile. *Environ Microbiol* 2016;**18**:1646–53.

Gutiérrez MH, Pantoja S, Tejos E *et al.* The role of fungi in processing marine organic matter in the upwelling ecosystem off Chile. *Mar Biol* 2011;**158**:205–19.

Gutiérrez MH, Vera J, Srain B *et al.* Biochemical fingerprints of marine fungi: implications for trophic and biogeochemical studies. *Aquat Microb Ecol* 2020;**84**:75–90.

Hassett BT, Borrego EJ, Vonnahme TR *et al.* Arctic marine fungi: biomass, functional genes, and putative ecological roles. *ISME J* 2019;**13**:1484–96.

Hassett BT, Gradinger R. Chytrids dominate arctic marine fungal communities. *Environ Microbiol* 2016;**18**:2001–9.

Hassett BT, Vonnahme TR, Peng X *et al.* Global diversity and geography of planktonic marine fungi. 2020;**63**. https://doi.org/10.1515/bot-2018-0113.

Hitchcock GL. A comparative study of the size-dependent organic composition of marine diatoms and dinoflagellates. *J Plankton Res* 1982;**4**:363–77.

Jennings DH, Burke RM. Compatible solutes–the mycological dimension and their role as physiological buffering agents. *New Phytol* 1990;**116**:277–83.
Jiao N, Herndl GJ, Hansell DA *et al*. Microbial production of recalcitrant dissolved organic matter: long-term carbon storage in the global ocean. *Nat Rev Microbiol* 2010;**8**:593–9.
Jønasdøttir SH. Effects of food quality on the reproductive success of *Acartia tonsa* and *Acartia hudsonica*: laboratory observations. *Mar Biol* 1994;**121**:67–81.
Kagami M, Helmsing NR, van Donk E. Parasitic chytrids could promote copepod survival by mediating material transfer from inedible diatoms. *Hydrobiologia* 2011;**659**:49–54.
Kagami M, Miki T, Takimoto G. Mycoloop: chytrids in aquatic food webs. *Front Microbiol* 2014;**5**:166.
Kilias ES, Junges L, Šupraha L *et al*. Chytrid fungi distribution and co-occurrence with diatoms correlate with sea ice melt in the Arctic Ocean. *Commun Biol* 2020;**3**. DOI: 10.1038/s42003-020-0891-7.
Lipson DA. The complex relationship between microbial growth rate and yield and its implications for ecosystem processes. *Front Microbiol* 2015;**6**:615.
Moal J, Martin-Jezequel V, Harris RP *et al*. Interspecific and intraspecific variability of the chemical-composition of marine-phytoplankton. *Oceanolog Acta* 1987;**10**:339–46.
Moloney CL, Field JG. General allometric equations for rates of nutrient uptake, ingestion, and respiration in plankton organisms. *Limnol Oceanogr* 1989;**34**:1290–9.
Mühlenbruch M, Grossart H-P, Eigemann F *et al*. Mini-review: phytoplankton-derived polysaccharides in the marine environment and their interactions with heterotrophic bacteria. *Environ Microbiol* 2018;**20**:2671–85.
Muńiz S, Lacarta J, Pata MP *et al*. Analysis of the diversity of substrate utilisation of soil bacteria exposed to Cd and earthworm activity using generalised additive models. *PLoS ONE* 2014;**9**:e85057.
Nidzieko NJ. Allometric scaling of estuarine ecosystem metabolism. *Proc Natl Acad Sci* 2018;**115**:6733–8.
Oksanen J. Blanchet FG Friendly M *et al*. Vegan: Community Ecology Package. Version 2.5-7. 2020.
Olsson PA. Signature fatty acids provide tools for determination of the distribution and interactions of mycorrhizal fungi in soil. *FEMS Microbiol Ecol* 1999;**29**:303–10.
Parrish CC, French VM, Whiticar MJ. Lipid class and fatty acid composition of copepods (*Calanus finmarchicus*, *C. glacialis*, *Pseudocalanus sp*., *Tisbe furcata* and *Nitokra lacustris*) fed various combinations of autotrophic and heterotrophic protists. *J Plankton Res* 2012;**34**:356–75.
Paton FM, Jennings DH. Effect of sodium and potassium chloride and polyols on malate and glucose 6-phosphate dehydrogenases from the marine fungus *Dendryphiella salina*. *Trans Br Mycol Soc* 1988;**91**:205–15.
Priest T, Fuchsm B, Amann R *et al*. Diversity and biomass dynamics of unicellular marine fungi during a spring phytoplankton bloom. *Environ Microbiol* 2021;**23**:448–63.
Prosser CL, Brown JR FA. Comparative Animal Physiology, Chapter 8. W. B. Saunders Co, 1961.
Raghukumar S. Origin and evolution of marine fungi. In: *Fungi in Coastal and Oceanic Marine Ecosystems*. Springer, 2017, 307–21.
Ray JL, Althammer J, Skaar KS *et al*. Metabarcoding and metabolome analyses of copepod grazing reveal feeding preference and linkage to metabolite classes in dynamic microbial plankton communities. *Mol Ecol* 2016;**25**:5585–602.
Scholz B, Küpper FC, Vyverman W *et al*. Chytridiomycosis of marine diatoms-the role of stress physiology and resistance in parasite-host recognition and accumulation of defense molecules. *Mar Drugs* 2017;**15**:26.
Slocombe SP, Ross M, Thomas N *et al*. A rapid and general method for measurement of protein in micro-algal biomass. *Bioresour Technol* 2013;**129**:51–7.
Slocombe SP, Zhang Q, Ross M *et al*. Unlocking nature's treasure-chest: screening for oleaginous algae. *Sci Rep* 2015;**5**:9844.
Sommer F, Stibor H, Sommer U *et al*. Grazing by mesozooplankton from Kiel Bight, Baltic Sea, on different sized algae and natural seston size fractions. *Mar Ecol Prog Ser* 2000;**199**:43–53.
Sommer U, Charalampous E, Genitsaris S *et al*. Benefits, costs and taxonomic distribution of marine phytoplankton body size. *J Plankton Res* 2017;**39**:494–508.
Stevenson LA, Alford RA, Bell SC *et al*. Variation in thermal performance of a widespread pathogen, the amphibian Chytrid fungus *Batrachochytrium dendrobatidis*. *PLoS ONE* 2013;**8**:e73830. https://doi.org/10.1371/journal.pone.0073830.
Tam L, Derry AM, Kevan PG *et al*. Functional diversity and community structure of microorganisms in rhizosphere and non-rhizosphere Canadian arctic soils. *Biodivers Conserv* 2001;**10**:1933–47. DOI: 10.1023/A:1013143503902.
Taube R, Fabian J, den Wyngaert S *et al*. Potentials and limitations of quantification of fungi in freshwater environments based on PLFA profiles. *Fung Ecol* 2019;**41**:256–68.
Taylor JD, Cunliffe M. Multi-year assessment of coastal planktonic fungi reveals environmental drivers of diversity and abundance. *ISME J* 2016;**10**:2118–28.
van Uden N, Castelo-Branco R. *Metschnikowiella zobellii* sp. nov. and *M. krissii* sp. nov., two yeasts from the Pacific Ocean pathogenic for *Daphnia magna*. *Microbiology* 1961;**26**:141–8.
Wickham H. *ggplot2: Elegant Graphics for Data Analysis*. Springer-Verlag New York, 2016, ISBN 978-3-319-24277-4.
Willers C, van Rensburg PJ, Claassens S. Phospholipid fatty acid profiling of microbial communities–a review of interpretations and recent applications. *J Appl Microbiol* 2015;**119**:1207–18.
Wilson AE, Sarnelle O, Tillmanns AR. Effects of cyanobacterial toxicity and morphology on the population growth of freshwater zooplankton: meta-analyses of laboratory experiments. *Limnol Oceanogr* 2006;**51**:1915–24.
Winter C, Bouvier T, Weinbauer MG *et al*. Trade-offs between competition and defense specialists among unicellular planktonic organisms: the "killing the winner" hypothesis revisited. *Microbiol Mol Biol Rev* 2010;**74**:42–57.
Worden AZ, Follows MJ, Giovannoni SJ *et al*. Rethinking the marine carbon cycle: factoring in the multifarious lifestyles of microbes. *Science* 2015;**347**:1257594.
Yeh HD, Questel JM, Maas KR *et al*. Metabarcoding analysis of regional variation in gut contents of the copepod *Calanus finmarchicus* in the North Atlantic Ocean. *Deep Sea Res Part II* 2020;**180**:104738.
Zak JC, Willig MR, Moorhead DL *et al*. Functional diversity of microbial communities: a quantitative approach. *Soil Biol Biochem* 1994;**26**:1101–8.